Jahn-Teller-induced crossover of the paramagnetic response in the singly valent e_g system $LaMn_7O_{12}$

R. Cabassi,[1,*] F. Bolzoni,[1] E. Gilioli,[1] F. Bissoli,[1] A. Prodi,[1] and A. Gauzzi[2]

[1]*Istituto dei Materiali per Elettronica e Magnetismo–CNR, Area delle Scienze, 43100 Parma, Italy*

[2]*Institut de Minéralogie et de Physique des Milieux Condensés, Université Pierre et Marie Curie–Paris 6 and CNRS, 75005 Paris, France*

(Received 29 October 2009; revised manuscript received 18 February 2010; published 9 June 2010)

We investigate the high-temperature magnetic and transport properties of $LaMn_7O_{12}$, which displays a similar perovskitelike structure and the same single-valent Mn^{3+} properties of $LaMnO_3$ but a much simpler Jahn-Teller (JT) distortion at $T_{JT}=650$ K. We find that the magnetic response of $LaMn_7O_{12}$ is similar to that of $LaMnO_3$ below T_{JT}, but strikingly different in the undistorted phase above T_{JT}, where the Curie-Weiss susceptibility is strongly suppressed. Electrical resistivity and thermopower measurements unveil a concomitant crossover from nonadiabatic to adiabatic small polaron regime. This suggests that the above suppression is due to low-spin electron-hole dimers formed by the e_g charge transfer between Mn sites and stabilized by the slow JT dynamics above T_{JT}.

DOI: 10.1103/PhysRevB.81.214412 PACS number(s): 71.30.+h, 61.50.Ks, 71.38.Ht

I. INTRODUCTION

In manganese oxides with perovskitelike ABO_3 structure, e.g., $LaMnO_3$ and related compounds, the Jahn-Teller (JT) distortion and the buckling of the MnO_6 octahedra are known to determine the diverse charge, spin, and orbital orderings[1] responsible for remarkable properties, such as the colossal magnetoresistance.[2] Namely, the Mn-O bond distance and Mn-O-Mn bond angle, ψ, are key control parameters of both real and virtual $3de_g$ charge transfers between Mn ions giving rise to the double- and superexchange interactions, respectively.[3] Despite intense studies, the link between the above distortions and the charge transport mechanism remains controversial even in simpler single-valent systems, where only Mn ions with a nominal 3+ charge are present. In the prototype compound $LaMnO_3$, it was experimentally found that the JT-induced e_g orbital ordering at $T_{JT}=750$ K upon cooling leads to an abrupt increase of the electrical resistivity, concomitant to a crossover from a temperature-independent behavior above T_{JT} to a thermally activated behavior of polaronic type below T_{JT}.[4] It was proposed that the enhanced conductivity above T_{JT} arises from charge transfer fluctuations between neighboring ions.[4] This transfer is expected to be driven by a ferromagnetic (FM) double-exchange interaction, in agreement with the observation of an increased Weiss constant in the magnetic susceptibility, $\chi(T)$. However, a conclusive test of this scenario is hindered by the presence of sizable JT local distortions in the pseudocubic phase above T_{JT},[5,6] which provides evidence of an ordering of the distorted MnO_6 octahedra at T_{JT}. It follows that T_{JT} is *not* a *proper* JT transition because a sizable distortion of the octahedra is present in both temperature regions. In order to elucidate the mechanism of charge transfer in single-valence systems, it would be interesting to study a system displaying a *proper JT transition* characterized by a sudden distortion of the octahedra uniquely driven by the JT effect and not masked by coexisting distortions of elastic origin (e.g., lattice mismatch between layers).

Here we report a successful study on $LaMn_7O_{12}$,[7] the counterpart of $LaMnO_3$ with *quadruple* perovskite $AA'_3B_4O_{12}$ structure.[8,9] Indeed, it was recently found[10] that $LaMn_7O_{12}$ undergoes a proper JT transition at $T_{JT}=650$ K, corresponding to a cubic to monoclinic distortion. This simple situation arises from the peculiar quadruple perovskite structure shown in Fig. 1, where the buckling of the BO_6 octahedra accommodates the lattice mismatch between the AO and BO layers without any distortion of the BO_6 octahedra. A further simplification with respect to ordinary ABO_3 perovskites is that the buckling angle, $\phi=180°-\psi$, turns out to be almost constant $\approx 45°$ and independent of temperature in all quadruple perovskites hitherto reported, including the AMn_7O_{12} family of interest here (A', B=Mn, A=Na,Ca,La,Pr,Bi.[7,11–17] Such unusually large ϕ value would be explained by the condition of maximum packing of the octahedra. The buckling is enabled by the JT distortion of the A' site, which leads to a doubling of the cubic unit cell parameter of ordinary perovskites. Note that, in the cubic $Im\bar{3}$ phase stable at sufficiently high T, the BO_6 octahedra are constrained to be regular by symmetry. A JT distortion of these octahedra appears only at T_{JT} in the monoclinic $I/2m$ phase, with no further distortions, as ϕ is constant. Finally, no oxygen defects are found in quadruple perovskites probably because these defects would destabilize the square-coordinated A' site. On the other hand, in ordinary perovs-

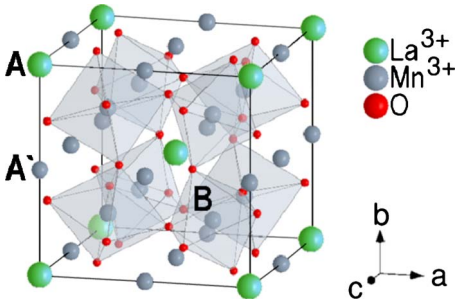

FIG. 1. (Color online) Crystal structure of the $Im\bar{3}$ cubic phase of $LaMn_7O_{12}$.

kites, any lattice mismatch inevitably leads to a distortion (typically orthorhombic *Pnma* of $GdFeO_3$-type) of the pristine cubic $Pm\bar{3}m$ structure because the A' site is absent. The resulting distortion is complex as the low site symmetry of the oxygens allows both, the buckling *and* the JT distortion of the BO_6 octahedra. The distortion pattern can be further complicated by local inhomogeneities and oxygen defects, as in the case of $LaMnO_3$.

In this work, we study the changes of magnetic and transport properties at T_{JT} in $LaMn_7O_{12}$. In view of the above considerations, our motivation is that the observed changes are unambiguously ascribed to the JT-driven distortion of the MnO_6 octahedra. The structural and physical properties of $LaMn_7O_{12}$ below room temperature were recently reported elsewhere.[7] The ground state is antiferromagnetic (AFM), similarly to that of $LaMnO_3$, which reflects the single-valent Mn^{3+} properties of both compounds. However, the AFM structure of the Mn^{3+} ions in the B sites is of C-type in $LaMn_7O_{12}$ and of A type in $LaMnO_3$. This difference is thought to reflect the presence of two different—instead of one—JT B sites in the unit cell and the larger buckling of the octahedra in $LaMn_7O_{12}$.[7] It was later reported[10] that the JT transition of $LaMn_7O_{12}$, concomitant to the above cubic-monoclinic transition, occurs at $T_{JT}=650$ K.

II. EXPERIMENTAL METHODS

$LaMn_7O_{12}$ powder samples were synthesized under high pressure using a multi-anvil apparatus as described in detail elsewhere.[7] Phase purity was checked by means of both x-ray and neutron powder diffraction. These measurements were carried out using a commercial X-ray Siemens D500 diffractometer equipped with a Cu K_α source and at the NIST Center for Neutron Research in Gaithersburg, USA, respectively. Our data analysis indicates that the samples typically are better than 97% pure. The secondary phases could not be unambiguously determined because of their modest concentrations. The most likely candidates are Mn_2O_3, Mn_3O_4, and $LaMnO_3$. As described below, the contribution of these impurities to the signal of the magnetic and transport measurements is negligible.

The magnetic and transport properties of the samples were investigated by means of dc magnetization (M), dc electrical resistivity (ϱ) and Seebeck coefficient (S) measurements as a function of temperature in the 200–800 K range. For these measurements, we used a commercial SQUID magnetometer equipped with a 5.5 T superconducting magnet and a high-temperature furnace. The dc electrical resistivity was measured in the four-probe (van der Pauw) configuration using a home-made sample-holder designed for the SQUID cryostat. The Seebeck coefficient was measured in the temperature range 300–800 K with a homemade apparatus.

III. RESULTS

A. Magnetic properties

Figure 2 shows the dc $M(T)$ curve of a high quality sample measured at 100 Oe. The data give evidence of a

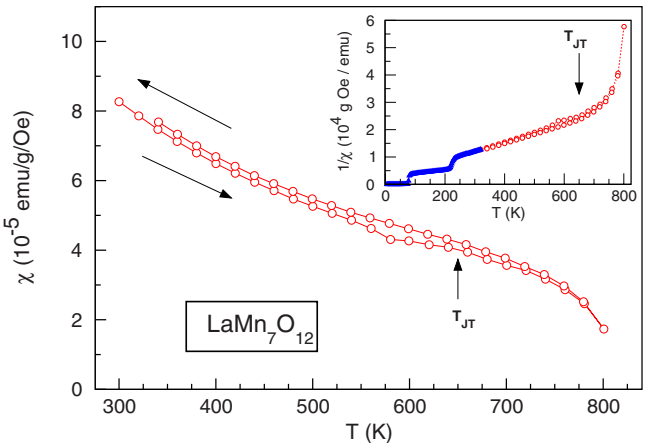

FIG. 2. (Color online) Temperature dependence of the magnetic susceptibility in the 300–800 K range of a $LaMn_7O_{12}$ sample measured at 100 Oe upon field cooling and field warming. Inset: inverse susceptibility data. The drop at 80 K is due to the antiferromagnetic transition of $LaMn_7O_{12}$ discussed in Ref. 7. The drop at 200 K is due to $LaMnO_{3+x}$ impurity (see text). Red and blue data points indicate two distinct data sets.

paramagnetic behavior consistent with previously reported low-T data.[7] The hysteresis at $T_{JT}=650$ K confirms the first-order structural phase transition observed by x-ray diffraction.[10] In the 250–700 K range, the linear behavior of the $\chi^{-1}(T)$ data in the inset of Fig. 2 gives evidence of Curie-Weiss behavior with effective moment $\mu=4.94$ (4.99) μ_B/Mn ion and Weiss constant $\theta=-57$ (-53) K upon cooling (warming). We checked the reproducibility of the data by measuring the same sample upon repeated thermal cycling up to high temperatures. This procedure enabled us to establish the stability of the $LaMn_7O_{12}$ phase up to 800 K.

The features of the $M(T)$ data at 80 and 200 K are not relevant here, as only the high temperature behavior is the object of our study. The drop at $T_{N,B}\simeq 80$ K corresponds to the AFM ordering of the B sublattice reported previously.[7] On the other hand, our systematic measurements on samples with different degrees of purity enabled us to attribute the drop at 200 K to the AFM transition of the $LaMnO_{3+x}$ (*viz* $La_{1-\epsilon}Mn_{1-\epsilon}O_3$) impurity, in agreement with previous studies of the effects of oxygen stoichiometry on this transition.[18–23] In the $\chi^{-1}(T)$ plot, the contribution of this impurity is more evident because $LaMnO_{3+x}$ is AFM-ordered in the $T_{N,B}-200$ K range, while $LaMn_7O_{12}$ is paramagnetic. A quantitative analysis of the $\chi(T)$ data in this range yields an estimate of the concentration of $LaMnO_{3+x}$ of less than 0.5%, which is negligible for our analysis of the magnetic response of $LaMn_7O_{12}$ in the high-temperature region of interest.

The μ values obtained from the previous data analysis are in agreement with the value 4.9 μ_B/ion expected for $S=2Mn^{3+}$ ions, which confirms the validity of the single-valent Mn^{3+} picture for $LaMn_7O_{12}$. The negative Weiss constant indicates a predominant AFM interaction, in agreement with the observation of AFM ordering of both A' and B sublattices by means of neutron diffraction.[7] The upturn of $\chi^{-1}(T)$ at T_{JT} is found to be fully reproducible upon thermal

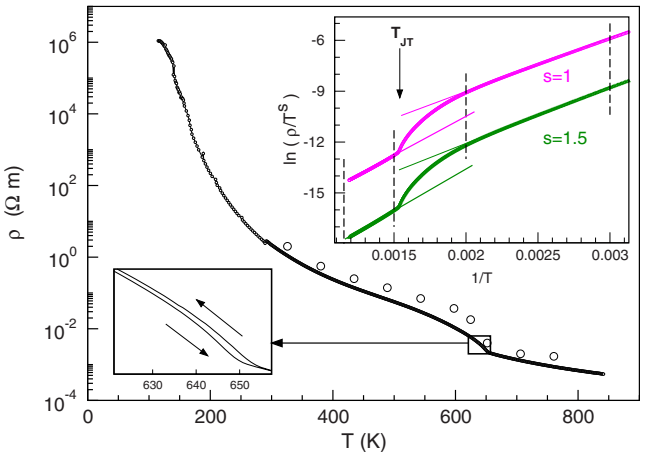

FIG. 3. (Color online) Solid line: electrical resistivity $\varrho(T)$ of $LaMn_7O_{12}$. Open circles: selected $\varrho(T)$ data of $LaMnO_{3.02}$ from Ref. 24 after rescaling of the temperature to the T_{JT} value of $LaMn_7O_{12}$. The rescaling puts into evidence the similar behavior of the two compounds. Upper inset: semilogarithmic $\varrho(T)$ vs $1/T$ plot showing the thermally activated behavior predicted by the small polaron scenario in both adiabatic ($s=1$) and nonadiabatic ($s=1.5$) regimes [see Eq. (1)]. Solid lines are linear fits of the data, dashed lines indicate the T ranges for the fit. Lower inset: detail of the thermal hysteresis in the vicinity of T_{JT}.

cycling up to 800 K, which indicates its intrinsic origin. We conclude that μ is significantly reduced in the cubic phase, where no JT distortion is present. It was previously reported[4] that the magnetic response of $LaMnO_3$ is described by a simple picture of paramagnetic Mn^{3+} ions both below and above T_{JT} with no change of μ but with an enhancement of the FM interaction arising from the double exchange mechanism above T_{JT}. Our results unveil a completely different scenario for $LaMn_7O_{12}$, where the above picture is appropriate only for the JT *distorted* structure, while a more complex picture is required for the cubic *undistorted* one.

B. Transport properties

The results of our dc electrical resistivity measurements are summarized in Fig. 3, where the transition at T_{JT} is clearly visible. Also these data exhibit a small—though clear—hysteresis at T_{JT}, which confirms the first order nature of this transition. It is worth to remark that these features of the $\varrho(T)$ data are found to be reproducible upon temperature cycling up to 850 K. We have successfully analyzed the data within the frame of a simple model of small polarons formed by the e_g electrons in the octahedral JT B sites. This model was put forward by a number of previous reports on $LaMnO_3$ as well as other doped manganese oxides displaying the CMR effect.[24–26]

For the quantitative analysis of the $\varrho(T)$ data, we remind that the transport of polarons consists of a thermally activated hopping described by the following expression[27,28]

$$\sigma = \sigma_0 \left(\frac{T_0}{T}\right)^s \exp\left(-\frac{E_\sigma}{k_B T}\right). \quad (1)$$

The above expression is valid in the $T > \Theta_D/2$ range, where Θ_D is the Debye temperature. The exponent is $s=1$ in the adiabatic regime, where the dynamical distortion of the lattice is slower than the hopping frequency. On the other hand, $s=1.5$ in the opposite (nonadiabatic) limit, where the dynamical distortions are faster than the hopping attempts.

TABLE I. Best-fit results of the analysis of the $\varrho(T)$ data within the small polaron picture in the adiabatic ($s=1$) and nonadiabatic ($s=1.5$) regimes (see text).

	E_σ (meV)	$\sigma_0 T_0^s$ (Ω^{-1} m^{-1} K^s)	Range for fit (K)
$T < T_{JT}$			[330;500]
Nonadiabatic regime	290	1.5×10^8	
Adiabatic regime	270	4.5×10^6	
$T > T_{JT}$			[670;840]
Nonadiabatic regime	430	1.8×10^{10}	
Adiabatic regime	400	4.0×10^8	

In order to establish the validity of the two regimes in our case, in the upper inset of Fig. 3 we reported the $\ln(\rho/T)$ and $\ln(\rho/T^{3/2})$ data in semilogarithmic scale as a function of inverse temperature in the $T > \Theta_D/2 \simeq 330$ K range, where Θ_D is the Debye temperature of $LaMn_7O_{12}$ reported previously.[7] A linear fit of these plots shows a very good agreement between the experimental data and the prediction of Eq. (1) in both adiabatic and nonadiabatic limits and in both temperature regions below and above T_{JT}. This shows the validity of the small polaron picture for $LaMn_7O_{12}$ both above and below the JT transition. The fit parameters are reported in Table I.

The above picture is supported by complementary thermopower measurements shown in Fig. 4. We analyzed these data using the following usual expression for the Seebeck coefficient $S(T)$, which is known to be valid in both cases of small polaron and band-gap semiconductor pictures:[29]

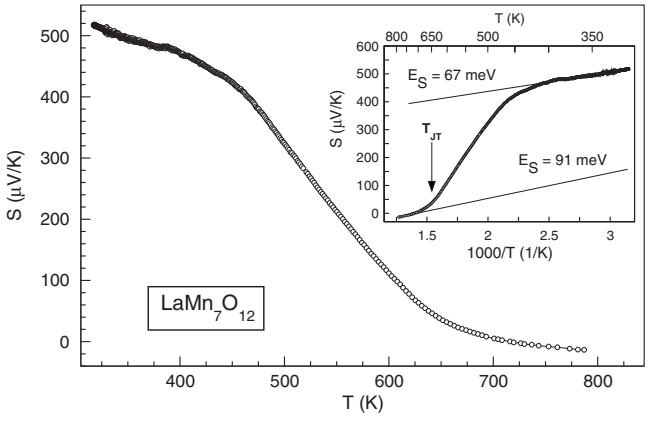

FIG. 4. Behavior of thermopower $S(T)$ in $LaMn_7O_{12}$. Inset: The same data plotted as a function of $1/T$, which yields $E_S \simeq 91$ meV (67 meV) above (below) T_{JT}.

$$S = \frac{E_S}{eT} + S_0. \quad (2)$$

In the case of small polaron transport, E_S is a characteristic energy smaller than the hopping activation energy E_σ, while the two energy scales are comparable in the case of band-gap semiconductors. Our data analysis yields $E_S \simeq 91$ meV (67 meV) above (below) T_{JT}. These values must be compared with the values $E_\sigma = 400$ meV (290 meV) obtained from the previous analysis of the $\varrho(T)$ data, and support therefore the small polaron picture in the whole T range of Figs. 3 and 4. We also note that the above value $E_\sigma \simeq 290$ meV below T_{JT} is exactly equal to the E_σ value reported for $LaMnO_3$. This confirms our previous remark on the similar transport mechanism in the two compounds in the JT distorted phase.

In order to differentiate between adiabatic and nonadiabatic regimes, we performed a linear fit of the $\ln(\rho/T)$ and $\ln(\rho/T^{3/2})$ data, as shown in the inset of Fig. 3. We found an equally good fit for both curves in both regions below and above T_{JT}, so our analysis has been further developed as shown below. According to a previous work,[30] in the adiabatic limit, the quantities σ_0 and T_0 in Eq. (1) are described as follows:

$$\sigma_0 = \frac{e^2}{ah} g_d c(1-c); \quad k_B T_0 = h\nu_0, \quad (3)$$

where a is the hopping distance, g_d is a geometric factor ranging from 1 to 5, c the carrier number per Mn site, and ν_0 is a characteristic phonon frequency. In the adiabatic regime ($s=1$), the prefactor $\sigma_0 T_0/T$ in Eq. (1) is directly obtained from Eq. (3) for $T \simeq T_0$. An estimate is obtained by taking a equal to the Mn-Mn distance $\simeq 0.37$ nm from Ref. 7. Assuming the adiabatic regime to be valid, we should then obtain $\sigma_0 T_0/T \simeq 10^5 g_d c(1-c)(\Omega\ \mathrm{m})^{-1}$. A lower value would indicate a slow hopping dynamics corresponding to the nonadiabatic regime. In order to estimate the value of $\sigma_0 T_0/T$ expected in the adiabatic regime, an estimate of c is needed. This is done by taking into account that the T-independent term S_0 in Eq. (2) is proportional to the derivative of the entropy with respect to the carrier number n:

$$S_0 = \frac{k_B}{|e|} \frac{\partial \ln g}{\partial n}, \quad (4)$$

where $n=cN$ with N the total site number, and g is the degeneracy of the electron ground state, which includes the configurational and the spin contributions. Various expressions for g have been previously proposed, depending on the particular physical system under consideration.[31–33] In our case, we should propose a dimer model, as described below. After some lengthy but straightforward algebra, one can derive an expression for g suitable for this model, and Eq. (4) becomes:

$$S_0 = \frac{k_B}{|e|}\left\{ \ln\left[\frac{(1-c)(1-2c)}{c}\right] + \ln(6) + \ln\left(\frac{24}{25}\right)\right\}. \quad (5)$$

By inserting the value of S_0 obtained from the linear fit of the high-temperature thermopower data into Eq. (5), we have $c \simeq 0.47$. One can thus obtain a quantitative estimate for $\sigma_0 T_0/T$, and finally compare it with the value obtained from the data fit of Table I, concluding that a crossover from nonadiabatic to adiabatic regime occurs at T_{JT} upon heating. This crossover indicates that the hopping process becomes comparatively faster than the JT dynamics above T_{JT}. We exclude that the hopping becomes faster, since the hopping activation energy is found to even increase above T_{JT} from $E_\sigma \approx 0.29$ eV to ≈ 0.40 eV. Therefore, we conclude that the JT dynamics in the high-T undistorted phase becomes much slower than in the low-T distorted phase. This also implies that the cubic structure is thermodynamically stable and does not result from averaged dynamic JT distortions of the lattice.

IV. DISCUSSION

The picture emerging from the previous analysis implies that the e_g electrons are localized even in the orbitally disordered phase above T_{JT}, contrary to the aforementioned case of $LaMnO_3$. The main consequence of this conclusion is that the hopping of such localized carriers leads to a dynamic charge disproportionation between neighboring Mn sites, by virtue of the single-valence properties of $LaMn_7O_{12}$. Since our previous analysis further indicates that, in the adiabatic regime above T_{JT}, the JT phonon dynamics is much slower than the hopping process, it follows that the disproportionated state should be stable within the time scale of the hopping process. A charge transfer mechanism was previously invoked also for the orbitally disordered phase of $LaMnO_3$. However, in that case, a picture of nearly delocalized carriers incompatible with the present small polaron picture was proposed. We argue that the case of $LaMn_7O_{12}$ is rather similar to the scenario proposed by Moskvin,[34] which predicts a disproportionated state described by the reaction $2MnO_6^{9-} \rightarrow MnO_6^{10-} + MnO_6^{8-}$ involving two neighboring MnO_6 complexes. This process leads to the formation of an electron-hole (EH) dimer behaving as a self-trapped d-d exciton. Since the EH dimer originates from two Mn^{3+} $S=2$ ions, the spin of the E-component of the dimer is $S_1 = 5/2$, while the spin of the H-component is $S_2 = 3/2$. Hence, the spin of the dimer can range from $S=1$ up to $S=4$ and its energy is $E_S = -\frac{1}{2} J_{\mathrm{eff}} S(S+1)$.

Our second point is that, provided the lifetime of the charge disproportionated state is longer than the JT dynamics, the EH dimer behaves as an effective boson. It is found[34] that the sign of J_{eff} is positive (negative) for sufficiently large (small) values of the superexchange hopping term, t. In $LaMn_7O_{12}$, t is comparatively small owing to the large buckling of the MnO_6 octahedra. Thus, the low-spin $S=1$ state would be favored, which corresponds to an effective moment considerably smaller than that of two Mn^{3+} ions in the conventional paramagnetic phase below T_{JT}. This simple scenario accounts for the observed suppression of magnetic susceptibility in $LaMn_7O_{12}$ above T_{JT}, although we do not exclude other scenarios that may account equally well for this suppression.

In conclusion, thanks to the simple JT distortion pattern of the quadruple perovskite structure, we could establish a di-

rect link between the JT distortion of the MnO_6 octahedra and the crossover of magnetic and transport behavior observed at T_{JT} in the single-valent Mn^{3+} system $LaMn_7O_{12}$. Such direct link cannot be established in the analog system $LaMnO_3$ and related compounds with ordinary perovskite structure because of the complex distortion pattern and the presence of oxygen defects characteristic of this structure. This crossover consists of a dramatic suppression of the Curie-Weiss susceptibility in the undistorted phase above T_{JT}, which is explained by a picture of long-lived electron-hole dimers formed by the charge transfer between neighboring Mn sites. Further studies by means of fast probes, such as resonant x-ray scattering,[34–36] would enable to probe this unusual electronic phase.

ACKNOWLEDGMENT

We gratefully acknowledge F. Licci and M. Marezio for stimulating discussions.

*cabassi@imem.cnr.it

[1] E. O. Wollan and W. C. Koehler, Phys. Rev. **100**, 545 (1955).
[2] R. von Helmolt, J. Wecker, B. Holzapfel, L. Schultz, and K. Samwer, Phys. Rev. Lett. **71**, 2331 (1993).
[3] J. B. Goodenough, *Magnetism and Chemical Bond* (Interscience, New York, 1963).
[4] J. S. Zhou and J. B. Goodenough, Phys. Rev. B **60**, R15002 (1999).
[5] M. C. Sánchez, G. Subías, J. García, and J. Blasco, Phys. Rev. Lett. **90**, 045503 (2003).
[6] X. Qiu, T. Proffen, J. F. Mitchell, and S. J. L. Billinge, Phys. Rev. Lett. **94**, 177203 (2005).
[7] A. Prodi, E. Gilioli, R. Cabassi, F. Bolzoni, F. Licci, Q. Huang, J. W. Lynn, M. Affronte, A. Gauzzi, and M. Marezio, Phys. Rev. B **79**, 085105 (2009).
[8] M. Marezio *et al.*, J. Solid State Chem. **6**, 16 (1973).
[9] B. Bochu *et al.*, J. Solid State Chem. **29**, 291 (1979).
[10] H. Okamoto, M. Karppinen, H. Yamauchi, and H. Fjellväg, Solid State Sci. **11**, 1211 (2009).
[11] A. Prodi, E. Gilioli, A. Gauzzi, F. Licci, M. Marezio, F. Bolzoni, Q. Huang, A. Santoro, and J. W. Lynn, Nature Mater. **3**, 48 (2004).
[12] B. Bochu, J. Chenavas, J. C. Joubert, and M. Marezio, J. Solid State Chem. **11**, 88 (1974).
[13] V. S. Rusakov, I. A. Presniakov, T. V. Gubaidulina, A. V. Sobolev, O. S. Volkova, G. Demazeau, A. V. Baranov, V. M. Cherepanov, and E. A. Gudilin, JETP Lett. **85**, 444 (2007).
[14] R. Przenioslo, I. Sosnowska, E. Suard, A. Hewat, and A. N. Fitch, Physica B **344**, 358 (2004).
[15] F. Mezzadri, M. Calicchio, E. Gilioli, R. Cabassi, F. Bolzoni, G. Calestani, and F. Bissoli, Phys. Rev. B **79**, 014420 (2009).
[16] F. Mezzadri, G. Calestani, M. Calicchio, E. Gilioli, F. Bolzoni, R. Cabassi, M. Marezio, and A. Migliori, Phys. Rev. B **79**, 100106(R) (2009).
[17] H. Okamoto, N. Imamura, M. Karppinen, H. Yamauchi, and H. Fjellväg, J. Solid State Chem. **183**, 186 (2010).
[18] J. Töpfer and J. B. Goodenough, J. Solid State Chem. **130**, 117 (1997).
[19] J. Töpfer and J. B. Goodenough, Chem. Mater. **9**, 1467 (1997).
[20] A. Tiwari and K. P. Rajeev, J. Mater. Sci. Lett. **16**, 521 (1997).
[21] M. Muroi and R. Street, Aust. J. Phys. **52**, 205 (1999).
[22] M. Verelst, N. Rangavittal, C. N. R. Rao, and A. Rousset, J. Solid State Chem. **104**, 74 (1993).
[23] P. A. Joy, C. Raj Sankar, and S. K. Date, J. Phys.: Condens. Matter **14**, 4985 (2002).
[24] J. A. Souza, J. J. Neumeier, R. K. Bollinger, B. McGuire, C. A. M. dos Santos, and H. Terashita, Phys. Rev. B **76**, 024407 (2007).
[25] P. Mandal, B. Bandyopadhyay, and B. Ghosh, Phys. Rev. B **64**, 180405(R) (2001).
[26] J. A. Souza, H. Terashita, E. Granado, R. F. Jardim, N. F. Oliveira, Jr., and R. Muccillo, Phys. Rev. B **78**, 054411 (2008).
[27] D. Emin and T. Holstein, Ann. Phys. (N.Y.) **53**, 439 (1969).
[28] I. G. Austin and N. F. Mott, Adv. Phys. **18**, 41 (1969).
[29] M. B. Salamon, Rev. Mod. Phys. **73**, 583 (2001).
[30] M. Jaime, H. T. Hardner, M. B. Salamon, M. Rubinstein, P. Dorsey, and D. Emin, Phys. Rev. Lett. **78**, 951 (1997).
[31] R. Heikes, in *Thermoelectricity*, edited by P. Egli (Wiley, New York, 1965).
[32] J. P. Dourmec, J. Solid State Chem. **110**, 419 (1994).
[33] P. M. Chaikin and G. Beni, Phys. Rev. B **13**, 647 (1976).
[34] A. S. Moskvin, Phys. Rev. B **79**, 115102 (2009).
[35] J. P. Attfield, Nature (London) **343**, 46 (1990).
[36] Y. Murakami, J. P. Hill, D. Gibbs, M. Blume, I. Koyama, M. Tanaka, H. Kawata, T. Arima, Y. Tokura, K. Hirota, and Y. Endoh, Phys. Rev. Lett. **81**, 582 (1998).